

1 Inter-annual variations of wet deposition in Beijing during 2014-2017:  
2 implications of below-cloud scavenging of inorganic aerosols

3

4 Baozhu Ge<sup>1,5\*</sup>, Danhui Xu<sup>1</sup>, Oliver Wild<sup>2</sup>, Xuefeng Yao<sup>3</sup>, Junhua Wang<sup>1,4</sup>, Xuechun  
5 Chen<sup>1</sup>, Qixin Tan<sup>1,4</sup>, Xiaole Pan<sup>1</sup>, Zifa Wang<sup>1,4,5\*</sup>

6 <sup>1</sup> State Key Laboratory of Atmospheric Boundary Layer Physics and Atmospheric  
7 Chemistry (LAPC), Institute of Atmospheric Physics (IAP), Chinese Academy of  
8 Sciences (CAS), Beijing 100029, China

9 <sup>2</sup> Lancaster Environment Centre, Lancaster University, LA1 4YQ, United Kingdom

10 <sup>3</sup> PLA 96941 Army, Beijing 102206, China

11 <sup>4</sup> University of Chinese Academy of Sciences, Beijing, 100049, China

12 <sup>5</sup> Center for Excellence in Regional Atmospheric Environment, Institute of Urban  
13 Environment, Chinese Academy of Sciences, Xiamen 361021, China

14 \*Correspondence to: Baozhu Ge ([gebz@mail.iap.ac.cn](mailto:gebz@mail.iap.ac.cn)) and Zifa Wang  
15 ([zifawang@mail.iap.ac.cn](mailto:zifawang@mail.iap.ac.cn))

16 **Abstract**

17 Wet scavenging is an efficient pathway for the removal of particulate matter (PM) from  
18 the atmosphere. High levels of PM have been a major cause of air pollution in Beijing  
19 but have decreased sharply under the Air Pollution Prevention and Control Action Plan  
20 launched in 2013. In this study, four years of observations of wet deposition have been  
21 conducted using a sequential sampling technique to investigate the detailed variation in  
22 chemical components through each rainfall event. We find that the major ions,  $\text{SO}_4^{2-}$ ,  
23  $\text{Ca}^{2+}$ ,  $\text{NO}_3^-$  and  $\text{NH}_4^+$ , show significant decreases over the 2013-2017 period (decreasing  
24 by 39%, 35%, 12% and 25%, respectively), revealing the impacts of the Action Plan.  
25 An improved method of estimating the below-cloud scavenging proportion based on  
26 sequential sampling is developed and implemented to estimate the contribution of  
27 below-cloud and in-cloud wet deposition over the four-year period. Overall, the below-  
28 cloud scavenging plays a dominant role to the wet deposition of four major ions at the  
29 beginning of the Action Plan. The contribution of below-cloud scavenging for  $\text{Ca}^{2+}$ ,  
30  $\text{SO}_4^{2-}$  and  $\text{NH}_4^+$  decreases from above 50% in 2014 to below 40% in 2017. This suggests  
31 that the Action Plan has mitigated PM pollution in the surface layer and hence decreased  
32 scavenging due to the washout process. In contrast, we find little change in the annual  
33 volume weighted average concentration for  $\text{NO}_3^-$  where the contribution from below-  
34 cloud scavenging remains at ~44% over the period 2015-2017. While highlighting the  
35 importance of different wet scavenging processes, this paper presents a unique new  
36 perspective on the effects of the Action Plan and clearly identifies oxidized nitrogen  
37 species as a major target for future air pollution controls.

38 **Key words:** wet scavenging, below-cloud, in-cloud, deposition,  $\text{PM}_{2.5}$

39

## 40 **1 Introduction**

41 Atmospheric wet deposition is a key removal pathway for air pollutants and is governed  
42 by two main processes: in-cloud and below-cloud scavenging (Goncalves et al., 2002;  
43 Andronache, 2003, 2004a; Henzing et al., 2006; Sportisse, 2007; Feng, 2009; Wang et  
44 al., 2010; Zhang et al., 2013). The below-cloud scavenging process depends both on  
45 the characteristics of the rain (snow), including the raindrop size distribution and  
46 rainfall rate, and on the chemical nature of the particles and their concentration in the  
47 atmosphere (Chate et al., 2003). Previously, below-cloud scavenging was thought to be  
48 less important than in-cloud processes and was simplified or even ignored in many  
49 global and regional chemical transport models (CTMs) (Barth et al., 2000; Tang et al.,  
50 2005; ENVIRON.Inc, 2005; Textor et al., 2006; Bae et al., 2010). However, more recent  
51 extensive research on wet scavenging has found that precipitation, even light rain, can  
52 remove 50-80% of the number or mass concentration of below-cloud aerosols, and this  
53 is supported by both field measurements and semi-empirical parameterizations of  
54 below-cloud scavenging in models (Andronache, 2004b; Zhang et al., 2004; Wang et al.,  
55 2014). Xu et al. (2017; 2019) studied the below-cloud scavenging mechanism based on  
56 the simultaneous measurement of aerosol components in rainfall and in the air in  
57 Beijing. They found that below-cloud scavenging coefficients for PM<sub>2.5</sub> widely used in  
58 CTMs ( $\sim 10^{-5}$ - $10^{-6}$ ) were 1-2 orders of magnitude lower than estimates from  
59 observations (at the range of  $10^{-4}$ - $10^{-5}$  for SO<sub>4</sub><sup>2-</sup>, NO<sub>3</sub><sup>-</sup> and NH<sub>4</sub><sup>+</sup>, respectively). This  
60 implies that the simulated below-cloud scavenging of aerosols might be significantly  
61 underestimated. This could be one reason for the underestimation of SO<sub>4</sub><sup>2-</sup> and NO<sub>3</sub><sup>-</sup>  
62 wet deposition in regional models of Asia reported in phase II and III of the Model  
63 Inter-Comparison Study for Asia (MICS-Asia) (Wang et al., 2008; Itahashi et al., 2020;  
64 Ge et al., 2020) and in global model assessments by the Task Force on Hemispheric  
65 Transport of Atmospheric Pollutants (TF-HTAP) (Vet et al., 2014), in addition to the  
66 other sources of model uncertainties (Chen et al., 2019; Tan et al., 2020; Kong et al.,  
67 2020), such as emissions, chemical transformation and changes in other ambient  
68 compounds of sulfur and nitrogen. Bae et al. (2012) added a new below-cloud  
69 scavenging parameterization scheme in the CMAQ model and improved the simulation

70 of aerosol wet deposition fluxes in East Asia by as much as a factor of two compared  
71 with observations. The below-cloud scavenging process is critical not only for wet  
72 deposition but also for the concentration of aerosols in the air and it should be  
73 represented appropriately in CTM simulations.

74 It is important to recognize the contribution of below-cloud scavenging to total wet  
75 deposition. However, many studies have found that it is difficult to separate the two wet  
76 scavenging processes based on measurement methods alone (Huang et al., 1995; Wang  
77 and Wang, 1996; Goncalves et al., 2002; Bertrand et al., 2008; Xu et al., 2017). A  
78 commonly used approach to separating below-cloud scavenging from total wet  
79 deposition is through sequential sampling (Aikawa et al., 2014; Ge et al., 2016; Aikawa  
80 and Hiraki, 2009; Wang et al., 2009; Quyang et al., 2015; Xu et al., 2017). In this way,  
81 precipitation composition during different stages of a rainfall event can be investigated  
82 separately in the lab after sampling. The chemical components in later increments of  
83 rainfall are thought to be less influenced by the below-cloud scavenging process than  
84 by the in-cloud scavenging process (Aikawa et al., 2014; 2009). Xu et al. (2017) applied  
85 this approach to summer rainfall in Beijing in 2014 and found that more than 50% of  
86 deposited sulfate, nitrate and ammonium ions were from below-cloud scavenging. In  
87 this study, an innovated method based on exponential curve to chemical ions in rainfall  
88 by sequential sampling is developed and implemented to estimate the ratio of below-  
89 cloud to in-cloud wet deposition in Beijing over the four-year period between 2014 and  
90 2017. Together with PM<sub>2.5</sub> concentration measurements, the below-cloud scavenging  
91 effects of the decreasing air pollutants at near-surface due to the Air Pollution  
92 Prevention and Control Action Plan (Action Plan) launched in 2013 (State Council of  
93 the People's Republic of China, 2019) is also investigated to explore the implications  
94 of the Action Plan to the precipitation chemistry.

## 95 **2 Data and methods**

### 96 **2.1 Measurement site and sampling methodology**

97 The measurement site is located on the roof of a two-floor building at the Institute of  
98 Atmospheric Physics tower site (IAP-tower, 39° 58' 28" N, 116° 22' 1" E) in northern  
99 Beijing. It is a typical urban site between the 3<sup>rd</sup> and 4<sup>th</sup> ring roads and lying close to

100 the Badaling expressway (Xu et al., 2017;2019;Sun et al., 2015). Four years of Inter-  
101 annual observations of each rainfall event were conducted at this site. Sequential  
102 sampling of each rainfall event is employed to catch the evolution of precipitation  
103 composition during each event. To investigate the detailed variation in the concentration  
104 of different chemical components in precipitation, especially the sharp changes  
105 occurring during the onset of rainfall, high resolution sampling of rainfall at 1 mm  
106 sequential increments was performed using an automatic wet-dry sampler. The  
107 rainwater collector uses a circular polyethylene board with a 30 cm diameter and  
108 collects up to eight fractions. About 70 ml of rainwater is collected for each of the first  
109 seven fractions and the rest of the rainfall is collected in the eighth fraction. For example,  
110 if there is 12 mm rainfall volume in a precipitation event, 1 mm sequential rainfall is  
111 collected in each of the first 7 fractions with the rest of 5 mm in the eighth fraction.  
112 Rainfall events where eight fractions are collected and identified as full events, and  
113 those with fewer than eight fractions are characterized as incomplete events. Manual  
114 sampling methods were used to collect more than eight fractions during heavy rainfall,  
115 and these are characterized as extended events. During 2014-2017, a total of 104  
116 precipitation events, which is almost 690 precipitation samples, were collected. Of the  
117 total number of precipitation events, 33 events (32%) were discarded from the  
118 sequential sampling analysis due to low rainfall amounts (<8 mm), which cannot satisfy  
119 the rules of full events. Altogether, 69 full events including 6 extended events were  
120 recorded over the 2014-2017 period in Beijing, as 15, 16, 20 and 18 events at each year,  
121 respectively. The rainfall volume of the eighth fraction of these 69 full events varied  
122 from 1 mm to 55.9 mm.

123 After collection, all samples are refrigerated at 0-4 °C and analyzed at the Key  
124 Laboratory for Atmospheric Chemistry, Chinese Academy of Meteorological Sciences  
125 (CAMS) within one month, following the procedure used for the Acid Rain Monitoring  
126 Network run by the China Meteorological Administration (CMA-ARMN) (Tang et al.,  
127 2007;2010). Nine ions that include four anions ( $\text{SO}_2^+$ ,  $\text{NO}_3^-$ ,  $\text{Cl}^-$  and  $\text{F}^-$ ) and five cations  
128 ( $\text{NH}_4^+$ ,  $\text{Na}^+$ ,  $\text{K}^+$ ,  $\text{Ca}^{2+}$  and  $\text{Mg}^{2+}$ ) are detected using ion chromatography (IC, Dionex  
129 600, USA). Their relative standard deviations in reproducibility tests are less than 5%.

130 Quality assurance is carried out using routine standard procedure of blind sample inter-  
131 comparison organized by CMA (Tang et al., 2010). Quality control is conducted by  
132 assessment of the anion-cation balance and by comparison of the calculated and  
133 measured conductivity. A more detailed description of the procedure can be found in  
134 Ge et al. (2016) and Xu et al. (2017).

## 135 **2.2 Aerosol measurements**

136 Aerosol mass concentration is recorded in routine measurements for the observation  
137 network of the China National Environmental Monitoring Center (CNEMC). PM<sub>2.5</sub>  
138 concentrations are used from the Olympic Park station, a monitoring station located 3  
139 km to the northeast of the IAP-tower sampling site. In addition, an Ambient Ion  
140 Monitor-Ion Chromatograph (AIM-IC) developed by URG Corp., Chapel Hill, NC and  
141 Dionex Inc., Sunnyvale, CA, is used to measure PM<sub>2.5</sub> composition at the sampling site  
142 between 2014 and 2017. This instrument includes a sample collection unit (URG 9000-  
143 D) for collection of water-soluble gases and particles in aqueous solution and a sample  
144 analysis unit (two ion chromatographs, Dionex ICS-2000 and ICS-5000) for analysis  
145 of both anions and cations. The limit of detection of AIM-IC is 0.08 mg/m<sup>3</sup> for NH<sub>4</sub><sup>+</sup>  
146 and 0.1 mg/m<sup>3</sup> for the other ions. Aerosol mass concentrations and composition are both  
147 measured at 1 h time resolution. Detailed descriptions of the AIM-IC instrumentation  
148 can be found in Malaguti et al. (2015) and Markovic et al. (2012). The average  
149 concentration of aerosols in the 6 h before each rainfall event is calculated to reflect the  
150 air pollution conditions before the event. For comparisons, the yearly average  
151 concentration of aerosols has been calculated to represent the normal conditions.

## 152 **2.3 Estimation of below cloud scavenging**

153 Previous studies have shown that the concentration of chemical ions in precipitation  
154 decreases through the progression of a rainfall event and eventually stabilizes at low  
155 levels (Aikawa and Hiraki, 2009;2014;Ge et al., 2016;Xu et al., 2017). The in-cloud  
156 and below-cloud scavenging contributions to total wet deposition are estimated based  
157 on the assumption that the concentrations in later increments can be attributed to  
158 scavenging by rainout only. This assumption relies on the efficient scavenging of air  
159 pollutants below cloud through the evolution of precipitation. However, the

160 concentration of chemical ions in precipitation may also be affected by many other  
161 factors in addition to below-cloud air pollutant concentrations and in-cloud scavenging  
162 processes. For example, the precipitation intensity may affect the scavenging efficiency  
163 of air pollutants below cloud and hence influence wet deposition (Andronache,  
164 2004b;Wang et al., 2014;Xu et al., 2017;2019). Yuan et al. (2014) reported that in  
165 central North China high intensity rainfall events of short duration (lasting less than 6  
166 h) are dominant rather than long-duration rainfall that is more common in the Yangtze  
167 River Valley. Therefore, the time window for the definition of in cloud stage is very  
168 important for estimating the below cloud and in cloud contributions. Previous studies  
169 have estimated the concentration of chemical ions scavenged in-cloud based on the  
170 judgment that 5 mm of accumulated precipitation is sufficient to identify the  
171 contribution of the in-cloud scavenging process (Wang et al., 2009;Aikawa and Hiraki,  
172 2009;Xu et al., 2017). Based on this approach, the concentration of  $\text{NO}_3^-$  and  $\text{SO}_4^{2-}$  in  
173 cloud in Japan was found to be 0.70 and 1.30 mg/L, respectively (Aikawa and Hiraki,  
174 2009). In Beijing, high concentration of  $\text{NH}_4^+$ ,  $\text{SO}_4^{2-}$  and  $\text{NO}_3^-$  during 2007 were found  
175 at 2.1~5.5, 3.1~14.9, 1.5~5.9 mg/L, respectively (Wang et al., 2009;Xu et al., 2017).

176 In this study, a new method based on fitting a curve to the chemical ion  
177 concentrations with successive rainfall increments has been developed to estimate the  
178 contribution of the in-cloud process. As shown in Figure 1, an exponential curve is  
179 fitted to the median, 25<sup>th</sup> and 75<sup>th</sup> percentiles of the chemical ion concentrations in each  
180 fraction through the rainfall increments. Noted that, the fitted exponential curve is  
181 applied to the combination of all 69 full events to estimate the yearly median  
182 concentration of chemical ions in-cloud and to compare with the results from previously  
183 reported method (i.e., median concentration after 5 mm increments). Besides, the  
184 exponential approach to each unique event was also employed. Ideally, the  
185 concentration of chemical ions stabilize at higher rainfall increments and this represents  
186 the concentration in cloud. However, the decrease during each rainfall event is distinctly  
187 different, and this regression method is not fully applicable to all rainfall events in  
188 practice. Therefore, the exponential regression method is used to estimate the in-cloud  
189 concentration under most circumstances, but where the decreasing trend with the

190 increment of rainfall is not significant, the average value of rainfall increments 6-8 of  
191 the event is used. The below cloud contributions to wet deposition of each species are  
192 then calculated using the following equations (1-2):

$$193 \quad \text{Wetdep}_{\text{below-cloud}} = \sum_{i=1}^n (C_i - \bar{C}) \times P_i \quad (1)$$

$$194 \quad \text{Contribution}_{\text{below-cloud}} = \frac{\text{Wetdep}_{\text{below-cloud}}}{\sum_{i=1}^n C_i \times P_i} \quad (2)$$

195 Where,  $C_i$ , and  $\bar{C}$  represent the concentration of each chemical ion in fraction  $i$  and in  
196 cloud and  $P_i$  represents the volume of rainfall, while  $n$  represent the total fractions in  
197 a rainfall event (equally to 8 in this study).

## 198 **3 Results and Discussion**

### 199 **3.1 Inter-annual variations in chemical components**

200 The Action Plan is launched in 2013 called “Ten rules” to improve the air quality in  
201 China. It includes comprehensive control of industrial emission, non-point emission,  
202 fugitive dust, vehicles, etc. It is also aimed to adjust and optimize the industrial  
203 structure and promote economic transformation and upgrading, such as increase the  
204 supply of clean energy. These actions are ensured to work by both of legislation and  
205 market mechanism. According to the *Beijing Environmental Statement* published by the  
206 Beijing Municipal Environmental Protection Bureau from 2013 to 2017, many  
207 measures have been implemented to meet the Action Plan, including replacement  
208 residential coal with electricity and natural gas, upgrading the emission standards of  
209 gasoline, diesel vehicles and power plants, closing the high-emission enterprises.  
210 Significant declines in atmospheric  $\text{PM}_{2.5}$  concentration have been observed nationwide  
211 between 2013 and 2017 during the Action Plan (Zhang et al., 2019). However, few  
212 studies have investigated the benefits of the Action Plan for wet deposition. A  
213 significant increase in  $\text{NO}_3^-$  in precipitation of 7.6% was observed at a regional  
214 background station in North China between 2003 and 2014 (Pu et al., 2017). A decrease  
215 in the ratio of  $\text{SO}_4^{2-}/\text{NO}_3^-$  mostly due to the decreasing of  $\text{SO}_4^{2-}$  and increasing of  $\text{NO}_3^-$   
216 suggests the transformation of sulfuric acid type to a mixed type of sulfuric and nitric  
217 acid in North China. However, the updated record especially after the Action Plan is  
218 important to assess the mitigation of the air pollutants not only in the atmosphere but



219 also in rainfall. A nationwide investigation of the wet deposition of inorganic ions in  
220 320 cities across China was recently made based on observations between 2011 and  
221 2016 from the National Acid Deposition Monitoring Network (NADMN), which was  
222 established by the China Meteorological Administration (Li et al., 2019). Briefly, both  
223  $\text{SO}_4^{2-}$  and  $\text{NO}_3^-$  across China experienced significant changes before and after 2014,  
224 with increases from 2011 to 2014 and then decreases from 2014 to 2016. In order to  
225 quantify the influence of the Action Plan on wet deposition in Beijing, four years of  
226 observations of each rainfall event are considered in this study. Figure 2 shows the  
227 volume weighted average (VWA) of inter-annual mean concentrations of  $\text{SO}_4^{2-}$ ,  $\text{NO}_3^-$ ,  
228  $\text{NH}_4^+$  and  $\text{Ca}^{2+}$  observed in Beijing during 2014 to 2017 along with those reported  
229 before 2010 from previous studies (Yang et al., 2012; Pan et al., 2012, 2013) (more  
230 detail is provided in Table S1 in supplementary materials). A continuous decrease in  
231 VWA concentrations between 1995 and 2017 is found for  $\text{SO}_4^{2-}$  and  $\text{Ca}^{2+}$ , with  
232 decreases of  $3.1\% \text{ yr}^{-1}$  and  $36.1\% \text{ yr}^{-1}$  in the earlier stage (1995-2010) and decreases of  
233  $9.8\% \text{ yr}^{-1}$  and  $8.8\% \text{ yr}^{-1}$  in the later stage (2014-2017). This is consistent with the annual  
234 changes in its emission and concentration as shown in Figure 3, in which the emission  
235 and the concentration data are collected from the yearly book of “*Environmental*  
236 *Bulletin in Beijing*” from 1994 to 2017. It is clearly shown the concentration of  $\text{SO}_2$   
237 experienced a sustainably decreasing trend due to significant reduction of its emission  
238 from 1996 to 2017, with the decreases rate is  $4.5\% \text{ yr}^{-1}$  and  $13.9\% \text{ yr}^{-1}$  in emission and  
239  $2.8\% \text{ yr}^{-1}$  and  $14.0\% \text{ yr}^{-1}$  in concentration during earlier stage and the later stage (the  
240 Action Plan period), respectively. For  $\text{NO}_3^-$  and  $\text{NH}_4^+$ , increases are found during the  
241 earlier stage (~60%) and decreases in the later stage (12% for  $\text{NO}_3^-$  and 25% for  $\text{NH}_4^+$ ).  
242 As to  $\text{NO}_x$  emission, the data in recent years have been collected. Although the clearly  
243 reduction is found in the annual changes of emission from 2010, the ambient  
244 concentration of  $\text{NO}_2$  do not show a significant decreasing trend ( $\sim 3.6\% \text{ yr}^{-1}$ ) compared  
245 with  $\text{SO}_2$  ( $14\% \text{ yr}^{-1}$ ). However, before the Action Plan, the decreasing ratio in  
246 concentration is only  $1.8\% \text{ yr}^{-1}$ , which is slower than the Action Plan period. Despite  
247 the increases of VWA  $\text{NO}_3^-$  in precipitation during the earlier stage, the small decreases  
248 in later stage would also be attributed to the Action Plan. All four components in the

249 later stage show significant decreases, suggesting that the Action Plan, which was  
250 implemented over this period, has a substantial impact. While  $\text{Ca}^{2+}$  and  $\text{SO}_4^{2-}$  played a  
251 prominent role in precipitation during the earlier stage before 2010,  $\text{NH}_4^+$  and  $\text{NO}_3^-$   
252 became the primary components in the later stage after 2010. It should be noted that  
253  $\text{NH}_4^+$  has a double role in environment pollution because it mitigates acid rain through  
254 neutralization, but also acidifies the soil by nitrification. Hence, while sulfur in  
255 precipitation has been further reduced under the Action Plan, additional attention is  
256 needed for nitrogen to prevent deterioration of the environment by acid rain resulting  
257 from nitrate and ammonium.

### 258 **3.2 Relationship in concentrations in precipitation and the atmosphere**

259 Wet deposition of a substance involves its removal from the associated air mass. The  
260 scavenging ratio  $H$  can be estimated by comparing the monthly average concentration  
261 in precipitation with that in the air (Okita et al., 1996;Kasper-Giebl et al., 1999;Hicks,  
262 2005;Yamagata et al., 2009). Xu et al. (Xu et al., 2017) first calculated the rainfall event  
263  $H$  based on the hourly concentration of aerosol components measured with an Aerodyne  
264 Aerosol Chemical Speciation Monitor (ACSM) and AIM-IC in 2014. In this study four  
265 years of observation of aerosol components have been undertaken by AIM-IC.  
266 Measurements made in the 6 hours before each rainfall event are averaged to represent  
267 the precondition of wet deposition precursors in the atmosphere. Figure 4 shows the  
268 relationship between the major chemical ions in precipitation and in the air. The VWA  
269 concentration of  $\text{SO}_4^{2-}$ ,  $\text{NO}_3^-$  and  $\text{NH}_4^+$  (hereafter SNA) as well as  $\text{Ca}^{2+}$  in each rainfall  
270 event has been calculated and compared with that in the first 1 mm rainfall fraction,  
271 F1#. As shown in Figure 4, positive correlations are found between the concentrations  
272 of ions in precipitation and in air, with Pearson correlation coefficients ( $R$ ) generally  
273 higher than 0.7 ( $p < 0.01$ ). The concentration in the first fraction should represent a high  
274 proportion of below-cloud scavenging due to the washout of air pollutants below clouds  
275 by the first rainfall, while the VWA represents a greater contribution from in-cloud  
276 removal (Aikawa and Hiraki, 2009;Wang et al., 2009;Xu et al., 2017). Thus, it is  
277 reasonable that the correlations are stronger for the first fraction than for the VWA, see  
278 Table 1. This indicates that the concentration of chemical ions in precipitation at the

279 start of rainfall is more greatly influenced by the air pollutants below the cloud. As  
280 rainfall continues and below-cloud concentrations are reduced, there is an increased  
281 contribution from in-cloud scavenging, which is less influenced by aerosols in the  
282 surface layer. This is confirmed by the substantial difference in the two R coefficients  
283 for the cation ion  $\text{Ca}^{2+}$  (0.85 for the first fraction, 0.47 for the VWA), which often exists  
284 in coarse particles below cloud. For the fine particle  $\text{SO}_4^{2-}$  which is present both in and  
285 below clouds (Xu et al., 2017), the difference in the two R coefficients is small. The R  
286 coefficients for  $\text{NO}_3^-$  and  $\text{NH}_4^+$  show less difference than  $\text{Ca}^{2+}$ , but larger difference  
287 than  $\text{SO}_4^{2-}$ . This may relate to their complicate sources from the ambient precursors.  
288 For example, the  $\text{NO}_3^-$  in precipitation is both from the fine and coarse particles (i.e.,  
289 particulate  $\text{NO}_3^-$ ) as well as the gaseous  $\text{HNO}_3$ , while the  $\text{NH}_4^+$  in precipitation is mainly  
290 from the fine particles in addition to  $\text{NH}_3$ .

291 The slope of the linear fits in Figure 4 can be used to calculate the scavenging ratio  
292  $W$ , which is the ratio of the ions concentration in precipitation (mg/L) and in air ( $\mu\text{g}/\text{m}^3$ ).  
293 The  $W$  ratio is  $0.25 \times 10^6$ ,  $0.16 \times 10^6$  and  $0.15 \times 10^6$  for SNA,  $\text{SO}_4^{2-}$ ,  $\text{NO}_3^-$  and  $\text{NH}_4^+$   
294 respectively. This is similar to that reported for rainfall events in 2014 in Beijing  
295 ( $0.26 \times 10^6$ ,  $0.35 \times 10^6$  and  $0.14 \times 10^6$  for SNA) by Xu et al. (2017) and consistent with  
296 those estimated in the eastern United States ( $0.11$ - $0.38 \times 10^6$ ,  $0.38$ - $0.97 \times 10^6$  and  $0.2$ -  
297  $0.75 \times 10^6$  for SNA) (Hicks, 2005). Compared with  $\text{SO}_4^{2-}$  and  $\text{NH}_4^+$ , the scavenging ratio  
298 for  $\text{NO}_3^-$  shows larger differences between this study and previous studies,  
299 corresponding to larger uncertainties to the R between the concentrations of ions in  
300 precipitation and in air for VWA in Figure 4a (lower significance  $p < 0.05$ ). It should be  
301 noted that the  $W$  calculated in this study is based on the fine particles in air, which  
302 may not represent the accurate reflection of the wet scavenging efficiency of SNA.

303 Wet deposition can affect much of the atmospheric column through in-cloud and  
304 below-cloud scavenging processes. The vertical column density (VCD) of  $\text{SO}_2$  and  $\text{NO}_2$   
305 from satellite during 2000s to 2017 is used here to compare with the inter-annual  
306 variations in wet deposition in Beijing (Figure S1). Consistent variation of the VCD  
307 and the yearly VWA concentration in precipitation is found in S and N. A continuous  
308 decrease is found in VCD  $\text{SO}_2$  from 2005 to 2017, matching the trend in  $\text{SO}_4^{2-}$

309 deposition, while for VCD NO<sub>2</sub> shows an increase from 2001 to 2011, a decrease after  
310 2011 and little change over the period 2014-2017. This implies that the Action Plan not  
311 only benefits air pollutants in the surface layer but also those in the total column. Due  
312 to faster decreases in emissions of S than N (Zheng et al., 2018), the ratio of S/N in both  
313 precipitation (SO<sub>4</sub><sup>2-</sup>/NO<sub>3</sub><sup>-</sup>, μeq/L) and air (SO<sub>4</sub><sup>2-</sup>/NO<sub>3</sub><sup>-</sup>, μg/m<sup>3</sup>) are found to decrease,  
314 with the change in ratio in precipitation at 17.5% yr<sup>-1</sup>, 11% yr<sup>-1</sup> and 20.0 % yr<sup>-1</sup> during  
315 1995-2010, 2014-2017 and 1995-2017, and in air at 12% yr<sup>-1</sup> during 2014-2017,  
316 respectively, see Figure S2. This is also consistent with the trend reported in whole  
317 China during 2000-2015 by Itahashi et al. (2018). The ratio of S/N in precipitation is a  
318 useful index to investigate the relative contributions of these acidifying species. In  
319 addition, the ratio of NH<sub>4</sub><sup>+</sup>/NO<sub>3</sub><sup>-</sup> is investigated here and a clear decrease is found during  
320 2014-2017 both in precipitation and in air. This indicates that NH<sub>4</sub><sup>+</sup> is decreasing faster  
321 than NO<sub>3</sub><sup>-</sup>. This evidence clearly confirms that nitrate should be the major target for air  
322 pollution controls in the next Action Plan.

### 323 **3.3 Proportion of below cloud scavenging**

324 As described in section 2.3, the in-cloud ion concentration ( $\bar{C}$ , in Eq 1) can be derived  
325 from the exponential fit of the observed rainwater concentrations. Table 2 lists the  
326 asymptote value and the exponential fitting equation of the evolution of each ion  
327 concentration in precipitation with the increment of rainfall. As shown, the asymptote  
328 value (here after, exponential approach) based on the median data for SO<sub>4</sub><sup>2-</sup>, NO<sub>3</sub><sup>-</sup> and  
329 NH<sub>4</sub><sup>+</sup> was 3.18 mg/L, 2.32 mg/L and 1.39 mg/L, respectively. The SO<sub>4</sub><sup>2-</sup> and NO<sub>3</sub><sup>-</sup> are  
330 within the range of reported in cloud concentrations for Beijing (3.33 mg/L and 2.75  
331 mg/L for SO<sub>4</sub><sup>2-</sup> and NO<sub>3</sub><sup>-</sup> in Xu et al., 2017), while the NH<sub>4</sub><sup>+</sup> in this study is lower than  
332 previous studies (2.51 mg/L in Xu et al., 2017 and 2.1-4.5 mg/L in Wang et al., 2009).  
333 In-cloud concentrations for other ions, i.e., Ca<sup>2+</sup>, F<sup>-</sup>, Cl<sup>-</sup>, Na<sup>+</sup>, K<sup>+</sup> and Mg<sup>2+</sup>, are 0.67  
334 mg/L, 0.04 mg/L, 0.27 mg/L, 0.1 mg/L, 0.06 mg/L and 0.08 mg/L, respectively. For  
335 comparison, the average concentration in fractions 6 to 8 (F6#~F8#) in each rainfall  
336 event (here after, average approach) is used to estimate the in-cloud concentration for  
337 events where successive rainwater concentrations do not show an obvious decrease or  
338 where other factors such as precipitation intensity are important, see Table 2. Similar

339 results are found for most ions with the exponential and average approach except for  
340  $\text{NH}_4^+$ ,  $\text{F}^-$ ,  $\text{K}^+$  and  $\text{Mg}^{2+}$ , where the maximum difference is less than 20% (Table 2). Thus,  
341 the replacement of in-cloud concentration by the average value is acceptable for  $\text{SO}_4^{2-}$ ,  
342  $\text{NO}_3^-$ ,  $\text{Ca}^{2+}$ ,  $\text{Cl}^-$  and  $\text{Na}^+$  but much uncertainty for the other ions. It is worth noting that  
343 for all ions the average approach gives higher estimates of in-cloud concentrations, and  
344 this can be recognized as an upper limit for in-cloud concentrations.

345 Following Eq (2), the contribution of below-cloud scavenging to wet deposition in  
346 each rainfall event during 2014-2017 are estimated from the in-cloud concentration.  
347 Figure 5 shows the yearly VWA of SNA and  $\text{Ca}^{2+}$  and the in-cloud and below-cloud  
348 contributions. The ratio of below-cloud contribution to the four major components  
349 based on the yearly median value of the in-cloud concentration is also shown in Figure  
350 5. Benefiting from the Action Plan, the air quality at the surface layer have been  
351 significantly improved (Zhang et al., 2019), which in turn leading to the decreases of  
352 the below-cloud scavenging. In this study, it also shows the below-cloud contributions  
353 of  $\text{SO}_4^{2-}$ ,  $\text{NO}_3^-$ ,  $\text{NH}_4^+$  and  $\text{Ca}^{2+}$  decreases from >50% in 2014 to ~40% in 2017. In 2017,  
354 the contribution of below-cloud scavenging declines to lower than 40% for  $\text{SO}_4^{2-}$  and  
355  $\text{NH}_4^+$ , but remains at 44% for  $\text{NO}_3^-$ . Over the four-year period 2014-2017, the average  
356 yearly wet deposition for all ions and the below-cloud wet scavenging contributions are  
357 given in Table 2. Similar to the concentrations in precipitation, the wet deposition of  
358  $\text{SO}_4^{2-}$ ,  $\text{NO}_3^-$ ,  $\text{NH}_4^+$  decreased from 21.5  $\text{kgS ha}^{-1} \text{ yr}^{-1}$ , 8.9 and 19.0  $\text{kg N ha}^{-1} \text{ yr}^{-1}$  during  
359 2007-2010 (Pan et al., 2012; 2013) to 11.4  $\text{kgS ha}^{-1} \text{ yr}^{-1}$  ( $3.42 \times 10^3 \text{ mg m}^{-2} \text{ yr}^{-1}$ ), 6.9 and  
360 16.7  $\text{kgN ha}^{-1} \text{ yr}^{-1}$  ( $3.05 \times 10^3$  and  $2.15 \times 10^3 \text{ mg m}^{-2} \text{ yr}^{-1}$ ) during 2014-2017, respectively.  
361 Below-cloud scavenging contributed to almost half of total deposition estimated with  
362 the exponential approach (50~60%), higher than the average approach (40~50%).

## 363 **4 Factors influencing below-cloud scavenging**

### 364 **4.1 Rainfall type**

365 The rainfall over the North China Plain in summer time is usually determined by the  
366 synoptic system such as the upper-level trough or the cold vortex. The 75 rainfall events  
367 have been classified based on synoptic system according to records from the Beijing  
368 Meteorological Service (<http://bj.cma.gov.cn>) with 33 events associated with upper-

369 level troughs, 23 events associated with a cold vortex and 19 events associated with  
370 other systems. Figure 6 shows the contributions of below-cloud scavenging for the two  
371 major systems. A high contribution from below-cloud scavenging is found for rainfall  
372 events associated with an upper-level trough with the median contributions for  $\text{SO}_4^{2-}$ ,  
373  $\text{NO}_3^-$ ,  $\text{NH}_4^+$  and  $\text{Ca}^{2+}$  of 56.2%, 62.1%, 56.3% and 61.9%, respectively. In the contrast,  
374 the contributions during rainfall events under cold vortex conditions are significant  
375 lower, with the values of 42.2%, 44.5%, 41.7% and 53.9%, respectively. Rainfall events  
376 associated with an upper-level trough are usually accompanied by orographic or frontal  
377 precipitation and are characterized by long and continuous precipitation (Shou et al.,  
378 2000). This suggests that below-cloud scavenging of chemical components is important  
379 for this rainfall type due to air mass transport from outside Beijing. In contrast, rainfall  
380 events associated with a cold vortex usually originate from strong thermal convection  
381 and are characterized by short heavy rainfall (Zhang et al., 2008; Liu et al., 2016; Zheng  
382 et al., 2020). This is common during the summer months in Beijing with deep  
383 convective clouds (Yu et al., 2011; Gao and He, 2013), and suggests that there is a large  
384 contribution from in-cloud scavenging to the total wet deposition.

#### 385 **4.2 Precipitation intensity and rainfall volume**

386 To illustrate the impacts of rainfall on below-cloud aerosol scavenging, the relationship  
387 between the below-cloud fraction and the rainfall volume and precipitation intensity are  
388 investigated, see Figure 7. Negative correlations in below cloud fraction are found for  
389 both the rainfall volume and precipitation intensity, although the relationship with the  
390 former is stronger ( $R$ : 0.63~0.93 vs. 0.03~0.64). This is consistent with results for 2014  
391 in Beijing reported by Xu et al. (2017). Atmospheric particles are efficiently removed  
392 below cloud by washout at the beginning of precipitation events (almost 70% of SNA  
393 is removed in the first 2-3 fractions, as shown in Figure 1). As the rainfall progresses,  
394 in-cloud scavenging makes an increasingly important contribution as below-cloud  
395 aerosol concentrations fall. Xu et al. (2017) found that heavy summertime rainfall  
396 events with more than 40 mm of rainfall usually occur over very short periods of time,  
397 usually 2-3 h. This heavy rainfall leads to the scavenging of aerosols in a relatively  
398 localized region and prevents the compensation associated with transport of air

399 pollutants from outside the region during longer-duration light rainfall events. This  
400 contributes to the decreased contribution of below-cloud scavenging during the high  
401 intensity rainfall events.

## 402 **5 Conclusions**

403 This paper presents an analysis of below-cloud scavenging from four years of  
404 sequential sampling of rainfall events in Beijing from May of 2014 to November of  
405 2017. The concentration of ions in precipitation varied dramatically, with yearly volume  
406 weighted averaged concentrations of  $\text{SO}_4^{2-}$ ,  $\text{NO}_3^-$ ,  $\text{NH}_4^+$  and  $\text{Ca}^{2+}$  decreasing by 39%,  
407 12%, 25% and 35% between 2014 and 2017, respectively. Due to faster decreases in  
408  $\text{SO}_4^{2-}$  than  $\text{NO}_3^-$  both in precipitation and in the air during the observation period, there  
409 is a significant decrease in S/N ratio in precipitation at 44% and in air at 48%.  
410 Benefiting from the national Air Pollution Prevention and Control Action Plan, the  
411 sulfur has been further reduced, while the nitrogen, especially nitrate, needs further  
412 attention in the next Action Plan to prevent deterioration of the environment associated  
413 with acid rain and photochemical pollution.

414 A new method has been developed and employed to estimate the below-cloud  
415 contribution to wet deposition in Beijing. The new approach suggests that the  
416 contribution from below-cloud scavenging is greater than that estimated applying  
417 simpler approaches used in previous studies. Overall, the contribution of below-cloud  
418 scavenging to the wet deposition of the four major components is important at 50~60%.  
419 The contribution of below-cloud scavenging shows a decrease over the period 2014-  
420 2017 for  $\text{Ca}^{2+}$ ,  $\text{SO}_4^{2-}$  and  $\text{NH}_4^+$ , but little change for  $\text{NO}_3^-$  during 2015-2017. Below-  
421 cloud scavenging also has a strong cleansing effect on air pollution, and the hourly  
422 concentration of  $\text{PM}_{2.5}$  is found to decrease sharply as the rainfall events occur, even  
423 with the effects from wind swept out have been accounted for.

424 Rainfall types also influence the contribution of below-cloud scavenging. Seventy-  
425 five rainfall events during the four-year periods were classified based on the local  
426 synoptic conditions. Lower contributions from below-cloud scavenging (~40%) are  
427 found for the four major ions in rainfall events associated with a cold vortex, while  
428 higher contributions (~60%) occurred associated with an upper-level trough.

429 Precipitation volume and intensity both show a negative correlation with the below-  
430 cloud fraction. This suggests that atmospheric particles are efficiently removed via  
431 below-cloud scavenging processes at the beginning of precipitation events. As the event  
432 progresses, rainfall in the later fractions shows a greater contribution from in-cloud  
433 scavenging processes as aerosols in the surface layer have already been removed. To  
434 better understand the mechanism of below-cloud scavenging processes, high resolution  
435 of measurement both in precipitation and in the air especially at the beginning of rainfall  
436 events are needed in the future.

437

#### 438 **Data availability.**

439 To request observed data for scientific research purposes, please contact Baozhu Ge at  
440 the Institute of Atmospheric Physics, Chinese Academy of Sciences, via email  
441 ([gebz@mail.iap.ac.cn](mailto:gebz@mail.iap.ac.cn)).

442

#### 443 **Author contribution**

444 BG and ZW designed the whole structure of this work, and prepared the manuscript  
445 with contributions from all co-authors. DX, XY, JW and QT helped with the data  
446 processing. OW, XC and XP was involved in the scientific interpretation and discussion.

447

#### 448 **Competing interests**

449 The authors declare that they have no conflict of interest

450

#### 451 **Acknowledgment**

452 We appreciate CNEMC for providing the data of the 6 criteria pollutants in Beijing. We  
453 also appreciate Beijing Municipal Environmental Monitoring Center for providing the  
454 aerosol components data in Beijing. This work is supported by the National Natural  
455 Science Foundation of China (Grant No 41877313, 91744206, 41620104008), Priority  
456 Research Program (XDA19040204) and the Key Deployment Program (ZDRW-CN-  
457 2018-1-03) of the Chinese Academy of Sciences.

458



459 **References:**

- 460 Aikawa, M., and Hiraki, T.: Washout/rainout contribution in wet deposition estimated  
461 by 0.5 mm precipitation sampling/analysis, *Atmos Environ*, 43, 4935-4939, 2009.
- 462 Aikawa, M., Kajino, M., Hiraki, T., and Mukai, H.: The contribution of site to washout  
463 and rainout: Precipitation chemistry based on sample analysis from 0.5 mm  
464 precipitation increments and numerical simulation, *Atmos Environ*, 95, 165-174,  
465 <http://dx.doi.org/10.1016/j.atmosenv.2014.06.015>, 2014.
- 466 Andronache, C.: Estimated variability of below-cloud aerosol removal by rainfall for  
467 observed aerosol size distributions, *Atmospheric Chemistry and Physics*, 3, 131-  
468 143, 2003.
- 469 Andronache, C.: Estimates of sulfate aerosol wet scavenging coefficient for locations  
470 in the Eastern United States, *Atmospheric Environment*, 38, 795-804,  
471 [10.1016/j.atmosenv.2003.10.035](http://dx.doi.org/10.1016/j.atmosenv.2003.10.035), 2004a.
- 472 Andronache, C.: Precipitation removal of ultrafine aerosol particles from the  
473 atmospheric boundary layer, *J Geophys Res-Atmos*, 109, 2004b.
- 474 Bae, S. Y., Jung, C. H., and Kim, Y. P.: Derivation and verification of an aerosol  
475 dynamics expression for the below-cloud scavenging process using the moment  
476 method, *J Aerosol Sci*, 41, 266-280, 2010.
- 477 Bae, S. Y., Park, R. J., Yong, P. K., and Woo, J. H.: Effects of below-cloud scavenging  
478 on the regional aerosol budget in East Asia, *Atmos Environ*, 58, p.14-22, 2012.
- 479 Barth, M. C., Rasch, P. J., Kiehl, J. T., Benkovitz, C. M., and Schwartz, S. E.: Sulfur  
480 chemistry in the National Center for Atmospheric Research Community Climate  
481 Model: Description, evaluation, features, and sensitivity to aqueous chemistry, *J*  
482 *Geophys Res-Atmos*, 105, 1387-1415, 2000.
- 483 Bertrand, G., Celle-Jeanton, H., Laj, P., Rangognio, J., and Chazot, G.: Rainfall  
484 chemistry: long range transport versus below cloud scavenging. A two-year study  
485 at an inland station (Opme, France), *J Atmos Chem*, 60, 253-271, 2008.
- 486 Chate, D. M., Rao, P. S. P., Naik, M. S., Momin, G. A., Safai, P. D., and Ali, K.:  
487 Scavenging of aerosols and their chemical species by rain, *Atmospheric*  
488 *Environment*, 37, 2477-2484, [10.1016/S1352-2310\(03\)00162-6](http://dx.doi.org/10.1016/S1352-2310(03)00162-6), 2003.
- 489 Chen, L., Gao, Y., Zhang, M., Fu, J. S., Zhu, J., Liao, H., Li, J., Huang, K., Ge, B.,  
490 Wang, X., Lam, Y. F., Lin, C. Y., Itahashi, S., Nagashima, T., Kajino, M., Yamaji,  
491 K., Wang, Z., and Kurokawa, J.: MICS-Asia III: multi-model comparison and  
492 evaluation of aerosol over East Asia, *Atmos. Chem. Phys.*, 19, 11911-11937,
- 493 Feng, J.: A size - resolved model for below - cloud scavenging of aerosols by snowfall,  
494 *Journal of Geophysical Research*, 114, [10.1029/2008jd011012](http://dx.doi.org/10.1029/2008jd011012), 2009.
- 495 Gao, Y., and He, L. F.: The phase features of a cold vortex over north China (in English  
496 abstract), *J Appl Meteor Sci*, 24, 704-713, 2013.
- 497 Ge, B., Wang, Z., Gbaguidi, A. E., and Zhang, Q.: Source Identification of Acid Rain  
498 Arising over Northeast China: Observed Evidence and Model Simulation, *Aerosol*  
499 *Air Qual Res*, 16, 1366-1377, [10.4209/aaqr.2015.05.0294](http://dx.doi.org/10.4209/aaqr.2015.05.0294), 2016.
- 500 Ge, B., Itahashi, S., Sato, K., Xu, D., Wang, J., Fan, F., Tan, Q., Fu, J. S., Wang, X.,  
501 Yamaji, K., Nagashima, T., Li, J., Kajino, M., Liao, H., Zhang, M., Wang, Z., Li,

502 M., Woo, J. H., Kurokawa, J., Pan, Y., Wu, Q., Liu, X., and Wang, Z.: MICS-Asia  
503 III: Multi-model comparison of reactive Nitrogen deposition over China, *Atmos.*  
504 *Chem. Phys. Discuss.*, 2020, 1-43, 10.5194/acp-2019-1083, 2020.

505 Goncalves, F. L. T., Ramos, A. M., Freitas, S., Dias, M. A. S., and Massambani, O.: In-  
506 cloud and below-cloud numerical simulation of scavenging processes at Serra Do  
507 Mar region, SE Brazil, *Atmos Environ*, 36, 5245-5255, 2002.

508 Gryspeerdt, E., Stier, P., White, B. A., and Kipling, Z.: Wet scavenging limits the  
509 detection of aerosol effects on precipitation, *Atmos. Chem. Phys.*, 15, 7557-7570,  
510 10.5194/acp-15-7557-2015, 2015.

511 Henzing, J. S., Olivie, D. J. L., and van Velthoven, P. F. J.: A parameterization of size  
512 resolved below cloud scavenging of aerosols by rain, *Atmospheric Chemistry and*  
513 *Physics*, 6, 3363-3375, 2006.

514 Hicks, B. B.: A climatology of wet deposition scavenging ratios for the United States,  
515 *Atmos Environ*, 39, 1585-1596, 2005.

516 Huang, M., Shen, Z., and Liu, S.: A study on the formation processes of acid rain in  
517 some areas of Southwest China (in Chinese), *Scientia Atmospherica Sinica*, 19, 359-  
518 366, 1995.

519 Itahashi, S., Yumimoto, K., Uno, I., Hayami, H., Fujita, S. I., Pan, Y., and Wang, Y.: A  
520 15-year record (2001–2015) of the ratio of nitrate to non-sea-salt sulfate in  
521 precipitation over East Asia, *Atmos. Chem. Phys.*, 18, 2835-2852, 10.5194/acp-18-  
522 2835-2018, 2018.

523 Itahashi, S., Ge, B., Sato, K., Fu, J. S., Wang, X., Yamaji, K., Nagashima, T., Li, J.,  
524 Kajino, M., Liao, H., Zhang, M., Wang, Z., Li, M., Kurokawa, J., Carmichael, G.  
525 R., and Wang, Z.: MICS-Asia III: overview of model intercomparison and  
526 evaluation of acid deposition over Asia, *Atmos. Chem. Phys.*, 20, 2667-2693,  
527 10.5194/acp-20-2667-2020, 2020.

528 Kasper-Giebl, A., Kalina, M. F., and Puxbaum, H.: Scavenging ratios for sulfate,  
529 ammonium and nitrate determined at Mt. Sonnblick (3106 m asl), *Atmos Environ*,  
530 33, 895-906, 1999.

531 Kong, L., Tang, X., Zhu, J., Wang, Z., Fu, J. S., Wang, X., Itahashi, S., Yamaji, K.,  
532 Nagashima, T., Lee, H. J., Kim, C. H., Lin, C. Y., Chen, L., Zhang, M., Tao, Z., Li,  
533 J., Kajino, M., Liao, H., Wang, Z., Sudo, K., Wang, Y., Pan, Y., Tang, G., Li, M.,  
534 Wu, Q., Ge, B., and Carmichael, G. R.: Evaluation and uncertainty investigation of  
535 the NO<sub>2</sub>, CO and NH<sub>3</sub> modeling over China under the framework of MICS-  
536 Asia III, *Atmos. Chem. Phys.*, 20, 181-202, 10.5194/acp-20-181-2020, 2020.

537 Li, R., Cui, L., Zhao, Y., Zhang, Z., Sun, T., Li, J., Zhou, W., Meng, Y., Huang, K., and  
538 Fu, H.: Wet deposition of inorganic ions in 320 cities across China: spatio-temporal  
539 variation, source apportionment, and dominant factors, *Atmos. Chem. Phys.*, 19,  
540 11043-11070, 10.5194/acp-19-11043-2019, 2019.

541 Liu, X. M., Zhang, M. J., Wang, S. J., Zhao, P. P., Wang, J., and Zhou, P. P.: Estimation  
542 and analysis of precipitation cloud base height in China (in english abstract),  
543 *Meteor Mon*, 42, 1135-1145, 2016.

544 Malaguti, A., Mircea, M., La Torretta, T. M. G., Telloli, C., Petralia, E., Stracquadanio,  
545 M., and Berico, M.: Comparison of Online and Offline Methods for Measuring

546 Fine Secondary Inorganic Ions and Carbonaceous Aerosols in the Central  
547 Mediterranean Area, *Aerosol Air Qual Res*, 15, 2641-2653, 2015.

548 Markovic, M. Z., VandenBoer, T. C., and Murphy, J. G.: Characterization and  
549 optimization of an online system for the simultaneous measurement of atmospheric  
550 water-soluble constituents in the gas and particle phases, *J Environ Monitor*, 14,  
551 1872-1884, 2012.

552 Okita, T., Hara, H., and Fukuzaki, N.: Measurements of atmospheric SO<sub>2</sub> and SO<sub>4</sub><sup>2-</sup>,  
553 and determination of the wet scavenging coefficient of sulfate aerosols for the  
554 winter monsoon season over the Sea of Japan, *Atmos Environ*, 30, 3733-3739,  
555 1996.

556 Ouyang, W., Guo, B. B., Cai, G. Q., Li, Q., Han, S., Liu, B., and Liu, X. G.: The washing  
557 effect of precipitation on particulate matter and the pollution dynamics of rainwater  
558 in downtown Beijing, *Sci Total Environ*, 505, 306-314, 2015.

559 Pan, Y. P., Wang, Y. S., Tang, G. Q., and Wu, D.: Wet and dry deposition of atmospheric  
560 nitrogen at ten sites in Northern China, *Atmos Chem Phys*, 12, 6515-6535, 2012.

561 Pan, Y. P., Wang, Y. S., Tang, G. Q., and Wu, D.: Spatial distribution and temporal  
562 variations of atmospheric sulfur deposition in Northern China: insights into the  
563 potential acidification risks, *Atmos Chem Phys*, 13, 1675-1688, 2013.

564 Pu, W. W., Quan, W. J., Ma, Z. L., Shi, X. F., Zhao, X. J., Zhang, L. N., Wang, Z. F.,  
565 and Wang, W. Y.: Long-term trend of chemical composition of atmospheric  
566 precipitation at a regional background station in Northern China, *Sci Total Environ*,  
567 580, 1340-1350, 2017.

568 Seinfeld, J. H., and Pandis, S. N.: *Atmospheric chemistry and physics: from air  
569 pollution to climate change*, Wiley, New York, 2006.

570 Shou, S. W., Zhu, Q. G., Lin, J. R., and Tang, D. S.: *The principles and methods of  
571 weather science[M]*, China Meteorological Press, Beijing, 76-81 pp., 2000.

572 Sportisse, B.: A review of parameterizations for modelling dry deposition and  
573 scavenging of radionuclides, *Atmospheric Environment*, 41, 2683-2698,  
574 10.1016/j.atmosenv.2006.11.057, 2007.

575 State Council of the People's Republic of China, Notice of the general office of the state  
576 council on issuing the air pollution prevention and control action plan.  
577 [http://www.gov.cn/zwggk/2013-09/12/content\\_2486773.htm](http://www.gov.cn/zwggk/2013-09/12/content_2486773.htm). Accessed 21 August  
578 2019.

579 Sun, Y. L., Wang, Z. F., Du, W., Zhang, Q., Wang, Q. Q., Fu, P. Q., Pan, X. L., Li, J.,  
580 Jayne, J., and Worsnop, D. R.: Long-term real-time measurements of aerosol  
581 particle composition in Beijing, China: seasonal variations, meteorological effects,  
582 and source analysis, *Atmos Chem Phys*, 15, 10149-10165, 2015.

583 Tan, J., Fu, J. S., Carmichael, G. R., Itahashi, S., Tao, Z., Huang, K., Dong, X., Yamaji,  
584 K., Nagashima, T., Wang, X., Liu, Y., Lee, H. J., Lin, C. Y., Ge, B., Kajino, M.,  
585 Zhu, J., Zhang, M., Liao, H., and Wang, Z.: Why do models perform differently on  
586 particulate matter over East Asia? A multi-model intercomparison study for MICS-  
587 Asia III, *Atmos. Chem. Phys.*, 20, 7393-7410, 10.5194/acp-20-7393-2020, 2020.

588 Tang, A. H., Zhuang, G. S., Wang, Y., Yuan, H., and Sun, Y. L.: The chemistry of  
589 precipitation and its relation to aerosol in Beijing, *Atmos Environ*, 39, 3397-3406,

590 DOI 10.1016/j.atmosenv.2005.02.001, 2005.

591 Tang, J. C. H. B., Yu, X. L., Wang, S., Yao, P., Lv, B., Xu, X. B., and Ding, G.:  
592 Evaluation of results of station inter-comparison with blind samples in Acid Rain  
593 Monitoring Network in China, *Meteoro. Monthly*, 33, 75–83, 2007 (in English  
594 abstract).

595 Tang, J., Xu, X., Ba, J., and Wang, S.: Trends of the precipitation acidity over China  
596 during 1992–2006, *Chinese. Sci. Bul.*, 5, 1800–1807, doi:10.1007/s11434-009-  
597 3618-1, 2010.

598 Textor, C., Schulz, M., Guibert, S., Kinne, S., Balkanski, Y., Bauer, S., Bernsten, T.,  
599 Berglen, T., Boucher, O., Chin, M., Dentener, F., Diehl, T., Easter, R., Feichter, H.,  
600 Fillmore, D., Ghan, S., Ginoux, P., Gong, S., Kristjansson, J. E., Krol, M., Lauer,  
601 A., Lamarque, J. F., Liu, X., Montanaro, V., Myhre, G., Penner, J., Pitari, G., Reddy,  
602 S., Seland, O., Stier, P., Takemura, T., and Tie, X.: Analysis and quantification of  
603 the diversities of aerosol life cycles within AeroCom, *Atmos Chem Phys*, 6, 1777-  
604 1813, 2006.

605 Vet, R., Artz, R. S., Carou, S., Shaw, M., Ro, C. U., Aas, W., Baker, A., Bowersox, V.  
606 C., Dentener, F., Galy-Lacaux, C., Hou, A., Pienaar, J. J., Gillett, R., Forti, M. C.,  
607 Gromov, S., Hara, H., Khodzher, T., Mahowald, N. M., Nickovic, S., Rao, P. S. P.,  
608 and Reid, N. W.: A global assessment of precipitation chemistry and deposition of  
609 sulfur, nitrogen, sea salt, base cations, organic acids, acidity and pH, and  
610 phosphorus, *Atmos Environ*, 93, 3-100, 2014.

611 Wang, W. X., and Wang, T.: On acid rain formation in China, *Atmos Environ*, 30, 4091-  
612 4093, 1996.

613 Wang, X., Zhang, L., and Moran, M. D.: Uncertainty assessment of current size-  
614 resolved parameterizations for below-cloud particle scavenging by rain, *Atmos.*  
615 *Chem. Phys.*, 10, 5685-5705, 10.5194/acp-10-5685-2010, 2010.

616 Wang, X., Zhang, L., and Moran, M. D.: Development of a new semi-empirical  
617 parameterization for below-cloud scavenging of size-resolved aerosol particles by  
618 both rain and snow, *Geosci Model Dev*, 7, 799-819, 10.5194/gmd-7-799-2014,  
619 2014.

620 Wang, Y., Xue, L. I., Li, Y. A. O., Yanan, Z., and Yuepeng, P. A. N.: Variation of pH and  
621 Chemical Composition of Precipitation by Multi-step Sampling in Summer of  
622 Beijing 2007 (in english abstract), 30, 2715-2721, 2009.

623 Wang, Z. F., Xie, F. Y., Sakurai, T., Ueda, H., Han, Z. W., Carmichael, G. R., Streets,  
624 D., Engardt, M., Holloway, T., Hayami, H., Kajino, M., Thongboonchoo, N.,  
625 Bennet, C., Park, S. U., Fung, C., Chang, A., Sartelet, K., and Amann, M.: MICS-  
626 Asia II: Model inter-comparison and evaluation of acid deposition, *Atmos Environ*,  
627 42, 3528-3542, 2008.

628 Xu, D., Ge, B., Chen, X., Sun, Y., Cheng, N., Li, M., Pan, X., Ma, Z., Pan, Y., and Wang,  
629 Z.: Multi-method determination of the below-cloud wet scavenging coefficients of  
630 aerosols in Beijing, China, *Atmos. Chem. Phys.*, 19, 15569-15581, 10.5194/acp-  
631 19-15569-2019, 2019.

632 Xu, D. H., Ge, B. Z., Wang, Z. F., Sun, Y. L., Chen, Y., Ji, D. S., Yang, T., Ma, Z. Q.,  
633 Cheng, N. L., Hao, J. Q., and Yao, X. F.: Below-cloud wet scavenging of soluble

634 inorganic ions by rain in Beijing during the summer of 2014, *Environ Pollut*, 230,  
635 963-973, 10.1016/j.envpol.2017.07.033, 2017.

636 Yamagata, S., Kobayashi, D., Ohta, S., Murao, N., Shiobara, M., Wada, M., Yabuki, M.,  
637 Konishi, H., and Yamanouchi, T.: Properties of aerosols and their wet deposition in  
638 the arctic spring during ASTAR2004 at Ny-Alesund, Svalbard, *Atmos Chem Phys*,  
639 9, 261-270, 2009.

640 Yang, F., Tan, J., Shi, Z. B., Cai, Y., He, K., Ma, Y., Duan, F., Okuda, T., Tanaka, S., and  
641 Chen, G.: Five-year record of atmospheric precipitation chemistry in urban Beijing,  
642 China, *Atmos Chem Phys*, 12, 2025-2035, DOI 10.5194/acp-12-2025-2012, 2012.

643 Yu, Z. Y., He, L. F., Fan, G. Z., Li, Z. C., and Su, Y. L.: The basic features of the severe  
644 convection at the background of cold vortex over north china (in English abstract),  
645 *J Trop Meteor*, 27, 89-94, 2011.

646 Yuan, W. H., Sun, W., Chen, H. M., and Yu, R. C.: Topographic effects on  
647 spatiotemporal variations of short-duration rainfall events in warm season of  
648 central North China, *J Geophys Res-Atmos*, 119, 11223-11234, 2014.

649 Zhang, C., Zhang, Q., Wang, Y., and Liang, X.: Climatology of warm season cold  
650 vortices in East Asia: 1979-2005, *Meteorol Atmos Phys*, 100, 291-301, 2008.

651 Zhang, L., Michelangeli, D. V., and Taylor, P. A.: Numerical studies of aerosol  
652 scavenging by low-level, warm stratiform clouds and precipitation, *Atmos Environ*,  
653 38, 4653-4665, <https://doi.org/10.1016/j.atmosenv.2004.05.042>, 2004.

654 Zhang, L., Wang, X., Moran, M. D., and Feng, J.: Review and uncertainty assessment  
655 of size-resolved scavenging coefficient formulations for below-cloud snow  
656 scavenging of atmospheric aerosols, *Atmospheric Chemistry and Physics*, 13,  
657 10005-10025, 10.5194/acp-13-10005-2013, 2013.

658 Zhang, Q., Zheng, Y. X., Tong, D., Shao, M., Wang, S. X., Zhang, Y. H., Xu, X. D.,  
659 Wang, J. N., He, H., Liu, W. Q., Ding, Y. H., Lei, Y., Li, J. H., Wang, Z. F., Zhang,  
660 X. Y., Wang, Y. S., Cheng, J., Liu, Y., Shi, Q. R., Yan, L., Geng, G. N., Hong, C. P.,  
661 Li, M., Liu, F., Zheng, B., Cao, J. J., Ding, A. J., Gao, J., Fu, Q. Y., Huo, J. T., Liu,  
662 B. X., Liu, Z. R., Yang, F. M., He, K. B., and Hao, J. M.: Drivers of improved  
663 PM<sub>2.5</sub> air quality in China from 2013 to 2017, *P Natl Acad Sci USA*, 116, 24463-  
664 24469, 2019.

665 Zheng, B., Tong, D., Li, M., Liu, F., Hong, C., Geng, G., Li, H., Li, X., Peng, L., Qi, J.,  
666 Yan, L., Zhang, Y., Zhao, H., Zheng, Y., He, K., and Zhang, Q.: Trends in China's  
667 anthropogenic emissions since 2010 as the consequence of clean air actions, *Atmos.*  
668 *Chem. Phys. Discuss.*, 2018, 1-27, 10.5194/acp-2018-374, 2018.

669 Zheng, Y. F., Wang L. W., and Du, J. Y.: Comparative Analysis of the Features of  
670 Precipitating and Nonprecipitating Ice Clouds in the BeijingTianjin-Hebei Region  
671 in Summer (in english abstract), *Climatic and Environmental Research*, 25, 77-89,  
672 10.3878/j.issn.1006-9585.2019.18091, 2020.

673

674

675 Table 1. Correlation of the concentrations of major ions in air in the six hours before  
676 rainfall with those in precipitation. Pearson correlation coefficients are presented for  
677 monthly volume weighted average (VWA) concentrations and for the first fraction (F1<sup>#</sup>)  
678 in each event.

	<b>SO<sub>4</sub><sup>2-</sup> (n=13)</b>	<b>NO<sub>3</sub><sup>-</sup> (n=14)</b>	<b>NH<sub>4</sub><sup>+</sup> (n=13)</b>	<b>Ca<sup>2+</sup> (n=9)</b>
VWA	0.70 <sup>a</sup>	0.53 <sup>b</sup>	0.65 <sup>a</sup>	0.47
F1 <sup>#</sup>	0.76 <sup>a</sup>	0.62 <sup>a</sup>	0.77 <sup>a</sup>	0.85 <sup>a</sup>

679 Note: "a" and "b" represent significant correlations at  $p < 0.01$  and  $p < 0.05$ , respectively.

680

681

682 Table 2. Exponential fitting for the concentrations of major ions in different fractions of rainfall, and the contribution of below-cloud scavenging  
 683 to total deposition.

Chemical component	Exponential Fitting for 50 <sup>th</sup> percentile <sup>a</sup>	R <sup>2</sup> (n=11)	Asymptote value (mg/L)	Below cloud % <sup>b</sup>	Average of F6#-F8# (mg/L)	Below cloud % <sup>c</sup>	Difference % <sup>d</sup>	Total wet deposition (mg/m <sup>2</sup> /yr)
SO <sub>4</sub> <sup>2-</sup>	y=3.17+10.28 e <sup>-0.51x</sup>	0.85	3.18	50%	3.33	48%	<3%	3423.3
NO <sub>3</sub> <sup>-</sup>	y=2.32+11.03 e <sup>-0.45x</sup>	0.81	2.32	59%	2.59	54%	<6%	3046.5
NH <sub>4</sub> <sup>+</sup>	y=1.39+5.81 e <sup>-0.28x</sup>	0.79	1.39	65%	1.95	51%	<9%	2149.5
Ca <sup>2+</sup>	y=0.67+6.81 e <sup>-0.6x</sup>	0.93	0.67	52%	0.72	48%	<6%	746.0
F <sup>-</sup>	y=0.04+0.24 e <sup>-0.34x</sup>	0.91	0.04	56%	0.05	40%	<10%	49.0
Cl <sup>-</sup>	y=0.27+2.2 e <sup>-0.6x</sup>	0.95	0.27	53%	0.29	50%	<5%	309.7
Na <sup>+</sup>	y=0.1+1.34 e <sup>-0.94x</sup>	0.91	0.10	64%	0.10	64%	<1%	150.6
K <sup>+</sup>	y=0.06+0.49 e <sup>-0.47x</sup>	0.89	0.06	64%	0.07	58%	<9%	89.8
Mg <sup>2+</sup>	y=0.08+0.81 e <sup>-0.4x</sup>	0.83	0.08	61%	0.11	46%	<13%	109.2

684 <sup>a</sup> fitting for the median of each fraction in different rainfall events; <sup>b</sup> below cloud portion calculated based on the fitting curve; <sup>c</sup> below cloud portion  
 685 calculated based on the average value of fractions 6 to 8 (F6#~F8#) in rainfall events; <sup>d</sup> difference in concentrations between adjacent 1 mm  
 686 increments after 5 mm accumulated precipitation.

687  
 688

689 **Figures and captions**

690 **Figure 1.** Concentrations of  $\text{SO}_4^{2-}$  (a),  $\text{NO}_3^-$  (b),  $\text{NH}_4^+$  (c) and  $\text{Ca}^{2+}$  (d) in each 1-mm  
691 fraction of rainfall (i.e., F1#, F2#, ...) over different rainfall events in the observation  
692 periods. The red line shows an exponential fitting using the 50<sup>th</sup> percentile of the data  
693 and the red shading indicates the range between the 25<sup>th</sup> and 75<sup>th</sup> percentiles.

694 **Figure 2.** Time series of annual volume weighted average (VWA) concentration of the  
695 four major components  $\text{NH}_4^+$  (a),  $\text{Ca}^{2+}$  (b),  $\text{SO}_4^{2-}$  (c) and  $\text{NO}_3^-$  (d) in precipitation in  
696 Beijing.

697 **Figure 3.** Annual changes in emission and concentration of  $\text{SO}_2$  and  $\text{NO}_x$  in Beijing,  
698 data is collected from the yearly book of “*Environmental Bulletin in Beijing*” from 1994  
699 to 2017.

700 **Figure 4.** Relationships between the concentration of  $\text{NO}_3^-$  (a),  $\text{SO}_4^{2-}$  (b),  $\text{NH}_4^+$  (c) and  
701  $\text{Ca}^{2+}$  (d) in precipitation and in air in the 6 h before each precipitation event. The red  
702 square and blue triangle represented the relationships between the concentration of ions  
703 in air with that in F1# and in VWA, respectively.

704 **Figure 5.** The annual volume weighted average below-cloud and in-cloud portion of  
705  $\text{SO}_4^{2-}$  (a),  $\text{Ca}^{2+}$  (b),  $\text{NO}_3^-$  (c), and  $\text{NH}_4^+$  (d) during 2014-2017. The ratio of annual  
706 median below-cloud contribution for each component is represented as the black line  
707 in each panel. The mark #M and #A in the ratio of below-cloud represent the estimation  
708 based on the median value and average value of in-cloud concentration in each year,  
709 while the first quartile and the third quartiles are also included in the figure.

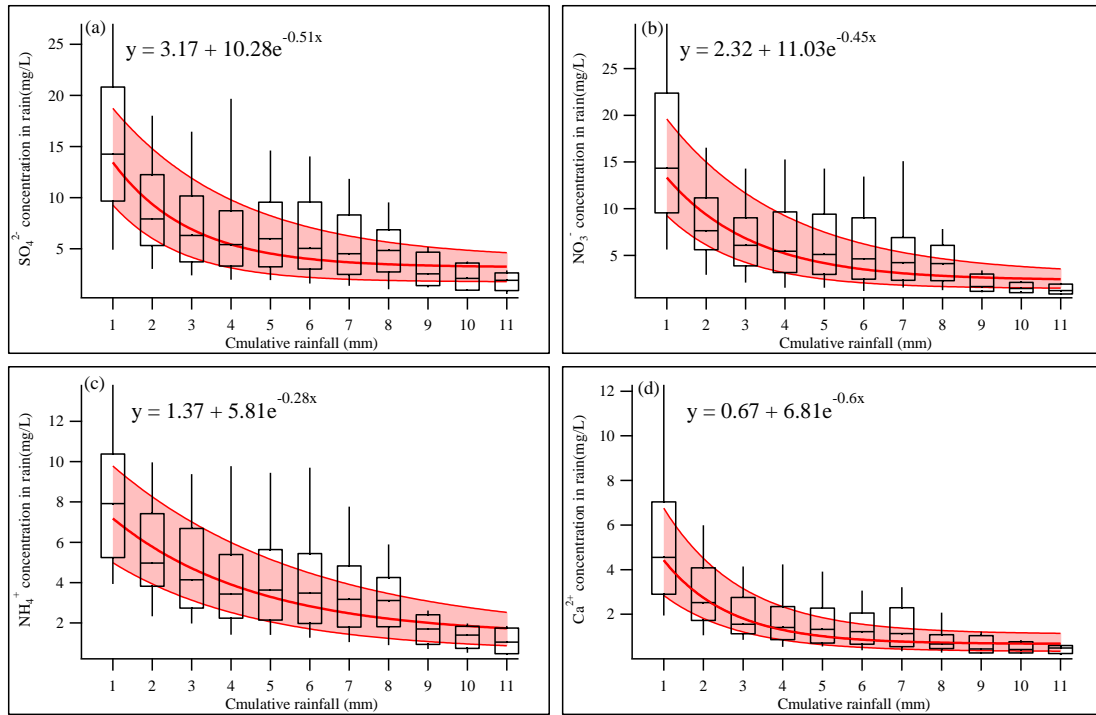
710 **Figure 6.** Contribution of below-cloud scavenging during rainfall events associated  
711 with different synoptic conditions.

712 **Figure 7.** Contribution of below-cloud scavenging in events with different rainfall  
713 volume and precipitation intensity

714

715



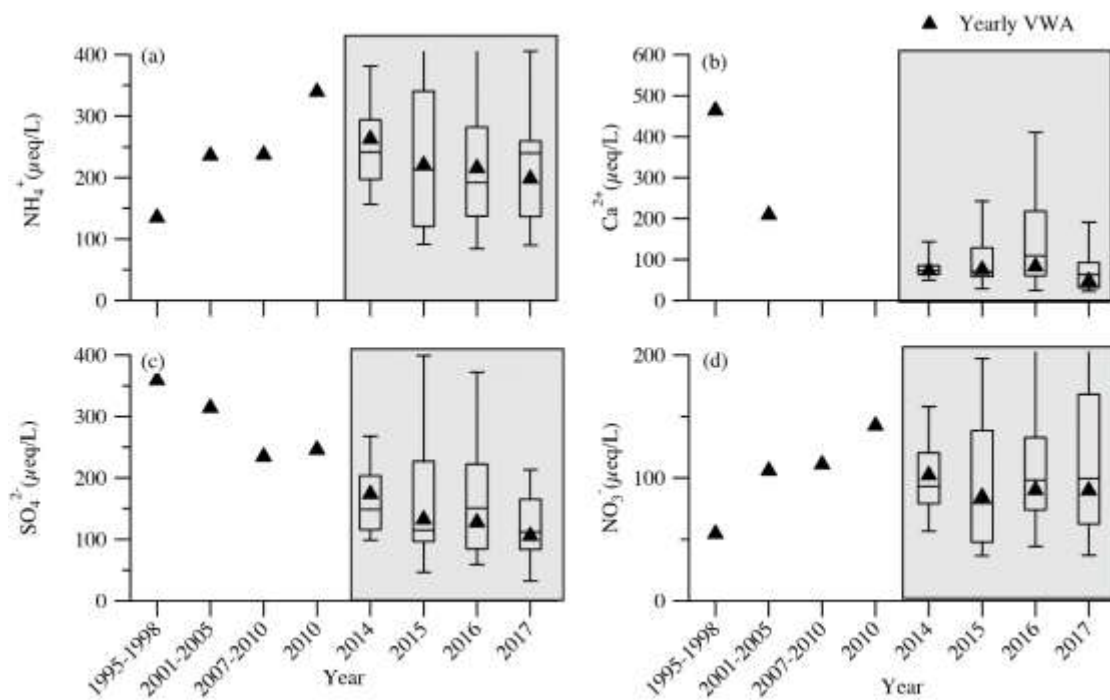


717

718 Figure 1. Concentrations of  $\text{SO}_4^{2-}$  (a),  $\text{NO}_3^-$  (b),  $\text{NH}_4^+$  (c) and  $\text{Ca}^{2+}$  (d) in each 1-mm  
 719 fraction of rainfall (i.e., F1#, F2#, ...) over different rainfall events in the observation  
 720 periods. The red line shows an exponential fitting using the 50<sup>th</sup> percentile of the data  
 721 and the red shading indicates the range between the 25<sup>th</sup> and 75<sup>th</sup> percentiles.

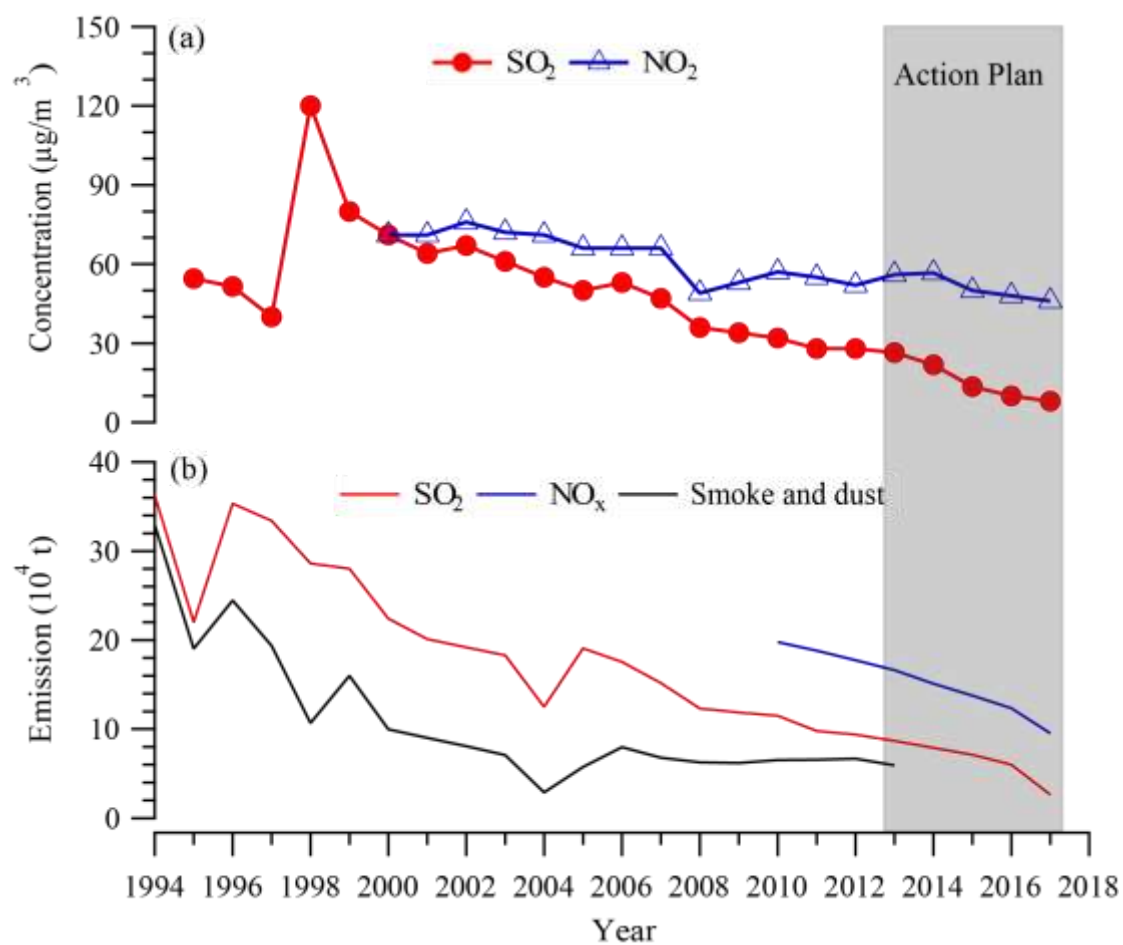
722

723



725

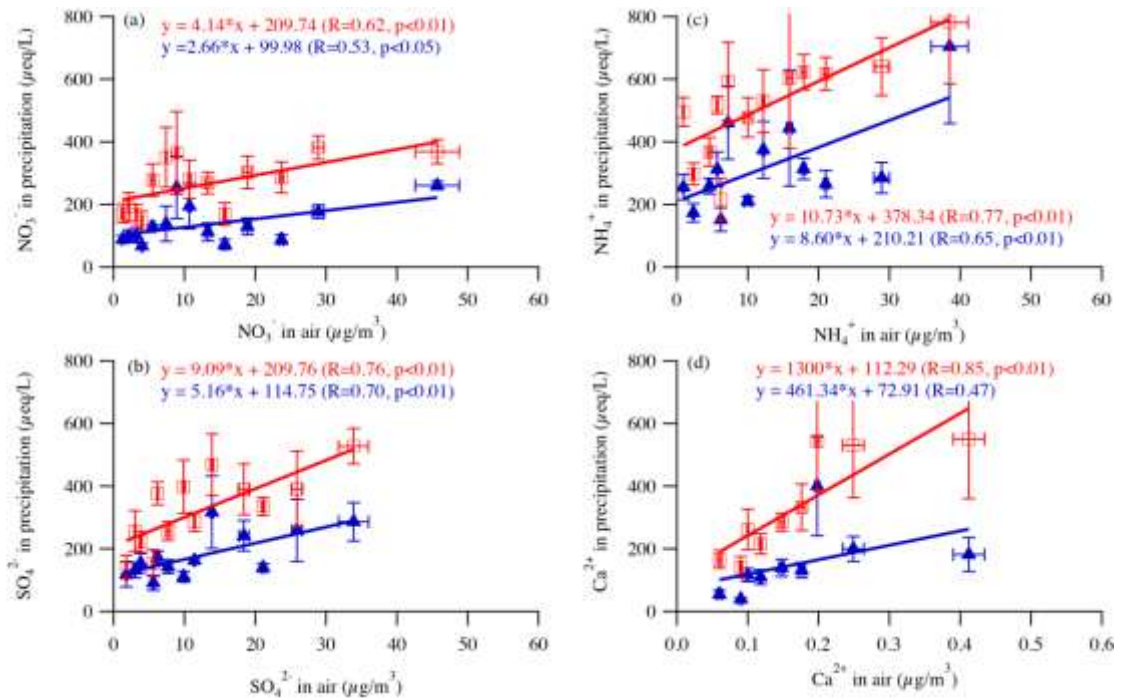
726 Figure 2. Time series of annual volume weighted average (VWA) concentration of the  
 727 four major components  $\text{NH}_4^+$  (a),  $\text{Ca}^{2+}$  (b),  $\text{SO}_4^{2-}$  (c) and  $\text{NO}_3^-$  (d) in precipitation in  
 728 Beijing.



730

731 Figure 3. Annual changes in emission and concentration of SO<sub>2</sub> and NO<sub>x</sub> in Beijing,  
 732 data is collected from the yearly book of “*Environmental Bulletin in Beijing*” from  
 733 1994 to 2017.

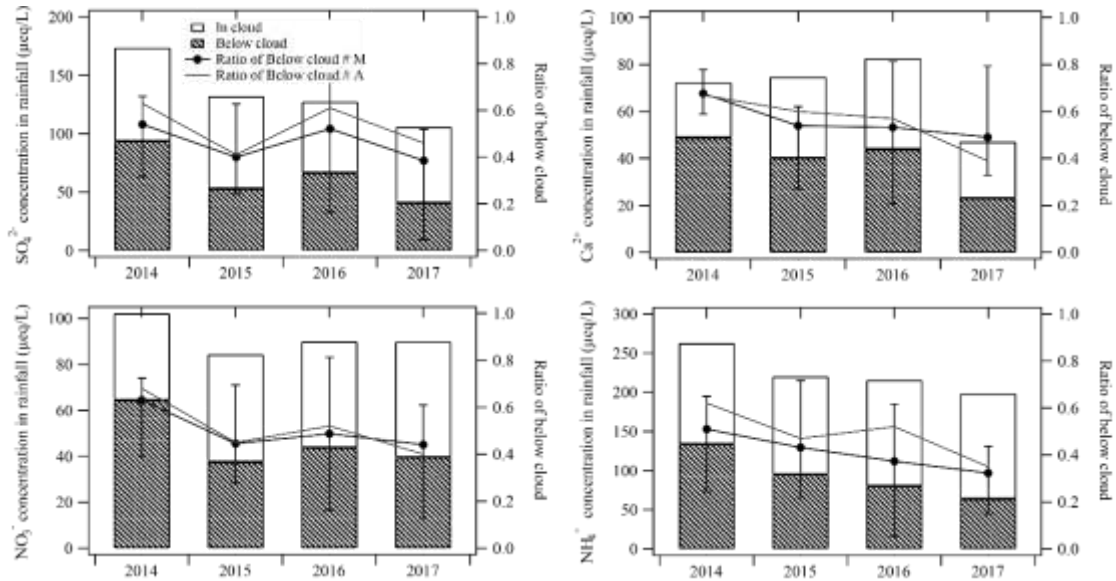
734



735

736 Figure 4. Relationships between the concentration of  $\text{NO}_3^-$  (a),  $\text{SO}_4^{2-}$  (b),  $\text{NH}_4^+$  (c) and  
737  $\text{Ca}^{2+}$  (d) in precipitation and in air in the 6 h before each precipitation event. The red  
738 square and blue triangle represented the relationships between the concentration of ions  
739 in air with that in F1# and in VWA, respectively.

740



741

742

743

744

745

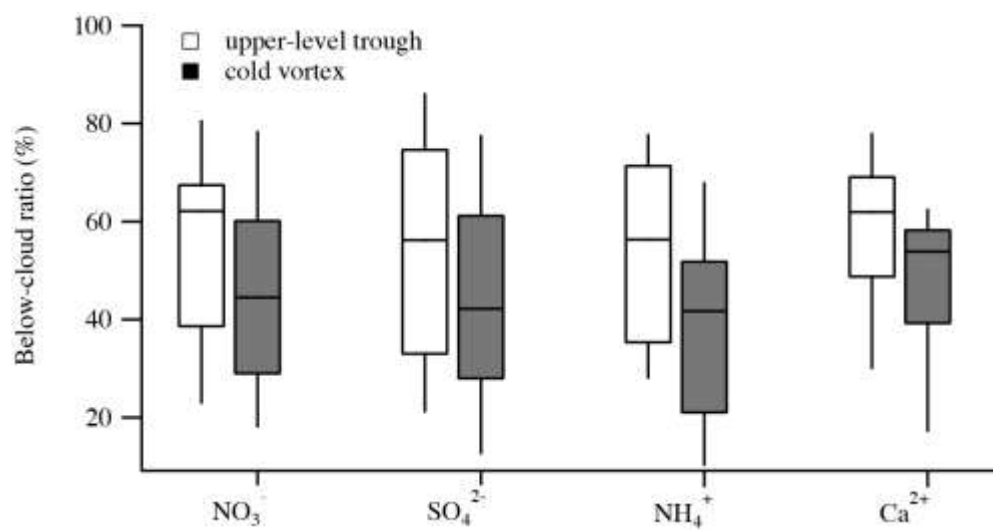
746

747

748

Figure 5. The annual volume weighted average below-cloud and in-cloud portion of  $\text{SO}_4^{2-}$  (a),  $\text{Ca}^{2+}$  (b),  $\text{NO}_3^-$  (c), and  $\text{NH}_4^+$  (d) during 2014-2017. The ratio of annual median below-cloud contribution for each component is represented as the black line in each panel. The mark #M and #A in the ratio of below-cloud represent the estimation based on the median value and average value of in-cloud concentration in each year, while the first quartile and the third quartiles are also included in the figure.

749

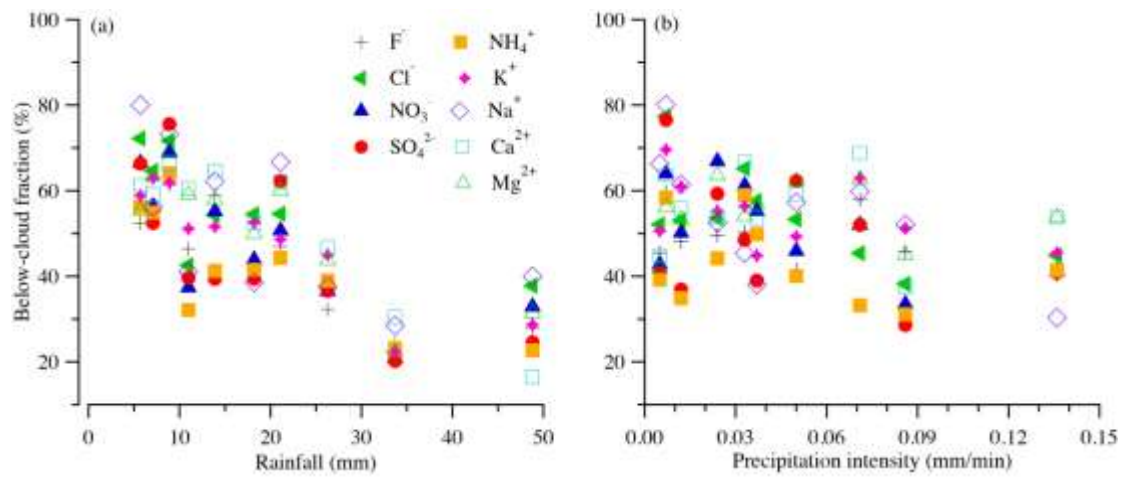


750

751 Figure 6. Contribution of below-cloud scavenging during rainfall events associated  
752 with different synoptic conditions.

753

754



755

756 Figure 7. Contribution of below-cloud scavenging in events with different rainfall  
757 volume and precipitation intensity.